Virology 443 (2013) 143–149

Contents lists available at SciVerse ScienceDirect

Virology

journal homepage: www.elsevier.com/locate/yviro

Multiple proviral integration events after virological synapse-mediated HIV-1 spread

Rebecca A. Russell [a,*,1], Nicola Martin [a,1], Ivonne Mitar [a], Emma Jones [b], Quentin J. Sattentau [a]

[a] The Sir William Dunn School of Pathology, The University of Oxford, South Parks Road, Oxford OX13RE, UK
[b] The Department of Medical Biochemistry and Immunology, Cardiff University School of Medicine, Cardiff CF14 4XN, Wales, UK

ARTICLE INFO

Article history:
Received 25 February 2013
Returned to author for revisions
21 March 2013
Accepted 3 May 2013
Available online 28 May 2013

Keywords:
HIV-1
Virological synapse
Integration

ABSTRACT

HIV-1 can move directly between T cells via virological synapses (VS). Although aspects of the molecular and cellular mechanisms underlying this mode of spread have been elucidated, the outcomes for infection of the target cell remain incompletely understood. We set out to determine whether HIV-1 transfer via VS results in productive, high-multiplicity HIV-1 infection. We found that HIV-1 cell-to-cell spread resulted in nuclear import of multiple proviruses into target cells as seen by fluorescence in-situ hybridization. Proviral integration into the target cell genome was significantly higher than that seen in a cell-free infection system, and consequent de novo viral DNA and RNA production in the target cell detected by quantitative PCR increased over time. Our data show efficient proviral integration across VS, implying the probability of multiple integration events in target cells that drive productive T cell infection.

Background

The human immunodeficiency virus type-1 (HIV-1) can spread with high efficiency by moving directly between infected and uninfected immune cells at the site of cell–cell contact, thereby obviating rate-limiting fluid-phase diffusion (Sattentau, 2008). This type of cell-to-cell movement has been studied in most detail in the principal HIV-1 target cell, the $CD4^+$ T lymphocyte, and functions predominantly via formation of intercellular contacts termed virological synapses (VS) (Sattentau, 2008). VS are related to, but distinct from, immunological synapses (Vasiliver-Shamis et al., 2009,2010,2008) and consist of polarized multimolecular structures containing adhesion molecules, viral envelope glycoproteins (Env) and viral receptors (Jolly et al., 2004; Piguet and Sattentau, 2004; Sattentau, 2008). Direct cell-to-cell movement of HIV-1 is more efficient than its cell-free counterpart (Chen et al., 2007; Martin et al., 2010; Mazurov et al., 2010; Sourisseau et al., 2007), and may be of particular significance in viral dissemination in secondary lymphoid tissues that are densely packed with $CD4^+$ T cells (Haase, 1999; Rudnicka et al., 2009). Both transmitted CCR5 tropic (R5) and CXCR4 tropic (X4) HIV-1 strains establish VS and spread in this way (Blanco et al., 2004; Hubner et al., 2009; Jolly et al., 2004; Martin et al., 2010; Ruggiero et al., 2008; Sourisseau et al., 2007). It has, however, been suggested that the observed viral uptake across the VS by endocytic mechanisms may not necessarily result in a productive infection (Blanco et al., 2004; Chen et al., 2007). Evidence for productive target cell infection across a VS consists of imaging the activation of a HIV-1 long terminal repeat driven fluorescent-expression cassette within the target cell (Ruggiero et al., 2008), activation of single cycle replication-dependent reporter vectors (Mazurov et al., 2010) and detection of de-novo synthesized viral DNA (Jolly et al., 2007a, 2007b; Martin et al., 2010) or viral Gag (Sourisseau et al., 2007) in infected-target cell conjugates. In additionDel Portillo et al. (2011) recently showed, using fluorescence in situ hybridization (FISH), that multiple proviral integration events occurred per cell as a result of transfer across VS. However, the fate of these integrants and the subsequent infection state of the target cells was not established.

The steps of viral infection of target cells via VS following HIV-1 genome reverse transcription, including nuclear import, integration and production of de-novo vRNA have not been dissected. This is in large part due to the technical difficulties implicit in studying new infectious events in a target cell that is closely associated with a previously infected donor cell. Here we have attempted to overcome these difficulties and further characterize the fate of viral nucleic acid in the target cell after cell-to-cell spread of HIV-1 using imaging and quantitative PCR assays and show that viral transfer across VS leads to proviral integration resulting in productive infection.

* Corresponding author. Fax: +44 1865 275515.
E-mail address: rebecca.moore@path.ox.ac.uk (R.A. Russell).
[1] These authors contributed equally to this work.

0042-6822/$ - see front matter © 2013 Published by Elsevier Inc.
http://dx.doi.org/10.1016/j.virol.2013.05.005

Results

VS-mediated HIV-1 spread results in transfer of multiple vDNA copies into the nucleus

In previous analyses we demonstrated that both X4 and R5 HIV-1 isolates assemble VS between contacting infected and uninfected, receptor-expressing T cells, resulting in de-novo synthesis of vDNA within target cells, and that this process is significantly more efficient than cell-free virus infection (Jolly et al., 2007a, 2007b; Martin et al., 2010). Although reverse transcription of incoming genomic RNA is an indicator of infection, most vDNA does not go on to integrate (Wu, 2008). Unintegrated vDNA is relatively unstable and is ultimately degraded or diluted from dividing cellular populations (Wu, 2008; Zhou et al., 2005). To investigate the steps in HIV-1 infection subsequent to reverse transcription following viral transfer across a VS, we carried out FISH on donor–target T cell conjugates. A VS formed between BaL-infected Jurkat.Tat.R5 cells (Jkt.R5$_{Ba-L}$) and target A301.R5 cells co-cultured for 1 h is shown in Fig. 1A, revealing the defining features that we previously demonstrated in VS formed by X4 HIV-1-infected T cells (Jolly et al., 2004), namely colocalization of Gag and Env on the donor cell and CD4 on the target cell. To establish the system of FISH for HIV-1-infected CD4$^+$ T cells, infected and uninfected T cell lines were cocultured to form VS as described above, then hybridized with probes generated from labelled fragmented vDNA either after treatment with RNase to eliminate intracellular vRNA, or without this treatment to reveal both vRNA and vDNA. Single optical sections were acquired for analysis: although this will modestly underestimate positive hybridization signals as it does not account for the entire nuclear volume, it eliminates false positives of FISH-labelled virions adherent to the plasma or nuclear membranes, or viral cores within the cytoplasm that superimpose over the nucleus. However, due to flattening of the cell and nucleus introduced by the FISH processing, we observed the majority of positive spots were within a single optical slice (data not shown) and so limited our analysis to this optical plane. Fig. 1B shows images from the ACH-2 T cell line containing 1 proviral copy per cell (Clouse et al., 1989) as a calibration control, and uninfected Jurkat cells and HIV-1 IIIB-infected Jurkat cells (Jkt$_{IIIB}$) as specificity controls. As anticipated, most ACH-2 cells (stained with cell tracker orange) revealed single spots suggestive of integrated provirus: the absence of spots in the remaining cells was most likely the result of the signal not being present in the nuclear volume imaged. Infected Jurkats contained multiple spots and no hybridization signal was detected

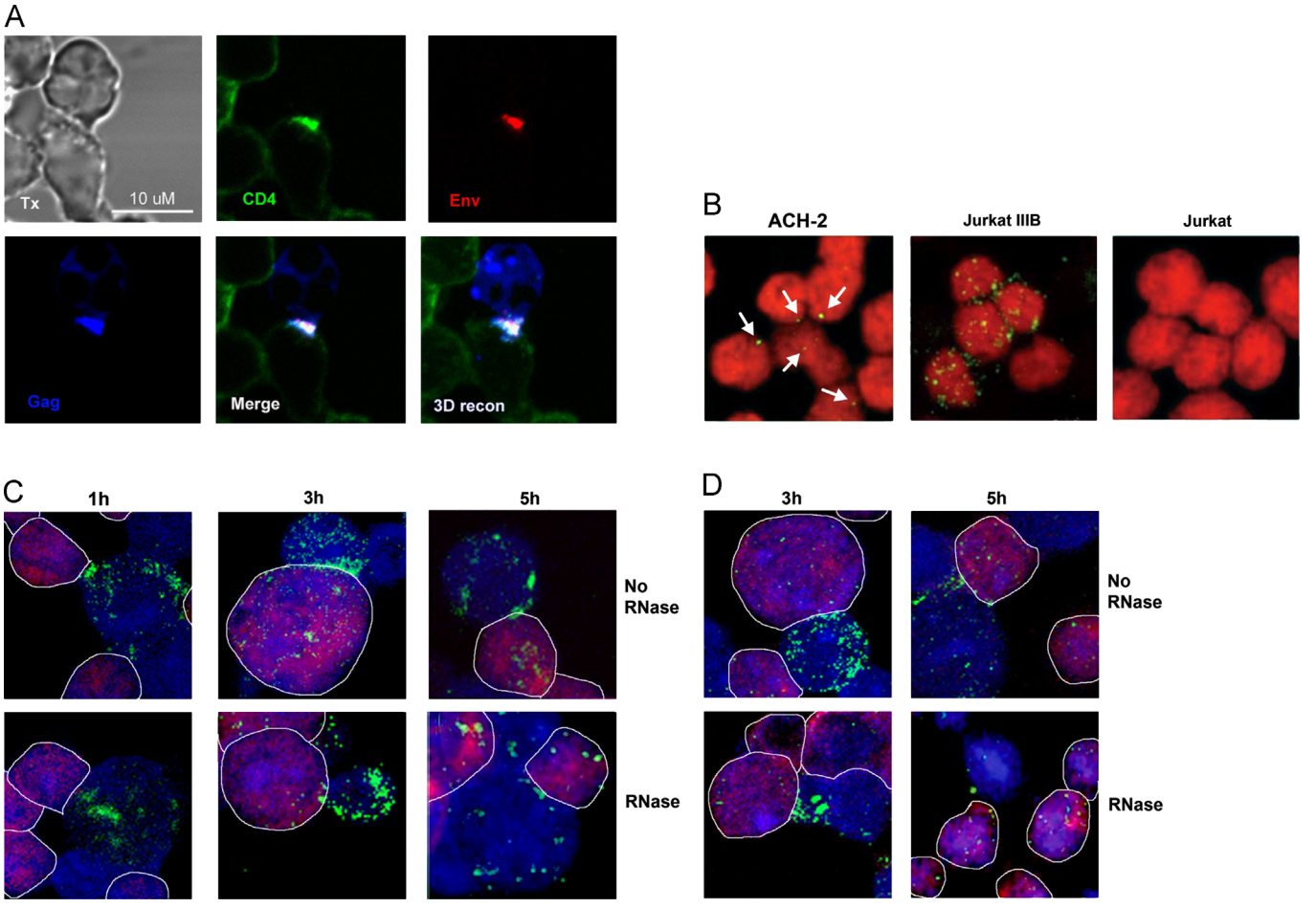

Fig. 1. Detection of HIV-1 antigens and nucleic acids in HIV-1 infected-target T cell conjugates. (A) The anatomy of the HIV-1$_{Ba-L}$ VS was probed by fixing conjugates of Jkt.R5$_{Ba-L}$ with A301.R5 cells formed over 1 h, staining with mAbs specific for CD4 and gp120 and polyclonal anti-Gag p17/p24 and taking single optical sections through the centre of the cells by LSCM. Single colours are shown for each label followed by all colours merged, and a three-dimensional reconstruction of *x*–*y* sections into a *z*-stack (3D recon). (B) 3D projections of FISH of vDNA in ACH-2 cells (left panel), Jkt$_{IIIB}$ (centre panel) and uninfected Jurkat cells (right panel). White arrows point to FISH signals. Cells are stained with CellTracker Orange. (C) 3D projections of FISH of conjugates of Jkt$_{IIIB}$-A301.R5 cells at the time points shown. Cell nuclei were labelled with TOTO-1 stain and are blue. Target A301.R5 cells were pre-labelled with Cell Tracker orange to differentiate them from the infected cells, and label is visualized as magenta. Top panel, total viral nucleic acids; bottom panel, vDNA only (RNase-treated). Target cells are outlined with a white border. (D) 3D projections of FISH of conjugates of Jkt.R5$_{BaL}$-A301.R5 cells at the time points shown. Cell nuclei and cytoplasm were labelled as for (C). Top panel, total viral nucleic acids; bottom panel, vDNA only (RNase-treated). Target cells are outlined with a white border.

in uninfected Jurkats, demonstrating the specificity of the system. To investigate the kinetics of viral nucleic acid transfer across VS, donor and target T cells mixed 1:1 were fixed at various times and probed. Target cells were distinguished by covalently labelling the cytoplasm with a stable fluorescent dye (orange), and all nuclei labelled with TOTO (blue) to confirm the nuclear localization of any FISH signal. To reveal total viral nucleic acid (vRNA and vDNA) transfer across VS, we carried out FISH in the absence of RNase treatment and analysed conjugates by laser scanning confocal microscopy (LSCM) with 3D Z stack projections. At 1 h a few conjugates had already formed, and a representative conjugate is shown in Fig. 1C (target cell is surrounded by a white boundary). Viral nucleic acid, most of which probably corresponds to genomic vRNA, was concentrated at the interfaces between the donor and target cells in the upper panels but no labelling was evident within the target cells. At 3 h multiple speckles had appeared in the target cell nuclei, and by 5 h distinct spots were observed. To visualize vDNA alone, samples were treated with RNase prior to FISH. At 1 h post-conjugate formation FISH signals corresponding to vDNA were observed in donor cells but not target cells (Fig. 1C lower panels). By 3 h small speckles colocalizing with target cell nuclei were observed and by 5 h obvious spots of label were evident within target cell nuclei, implying transfer of multiple proviral DNAs with the potential for integration. For HIV-$1_{Ba\text{-}L}$ we had previously observed slower transfer kinetics (Martin et al., 2010) and therefore we imaged the cells only at 3 and 5 h. We saw a few vDNA spots in target cells at 3 h and multiple vDNA spots at 5 h post-conjugate formation (Fig. 1D). To quantify the level of viral transfer across a VS resulting in vDNA production and nuclear import, target cells containing positive nuclear hybridization signals of RNase-resistant material were counted. At 1 h the number of positive target cells was not significantly above background (Fig. 2A). However by 3 h ~15% of target cells contained a positive FISH signal ($p < 0.05$), reducing to ~13% at 5 h ($p < 0.05$). The number of vDNA spots per infected target cell nucleus was also determined. The mean number of spots at 3 h was 3.4 with a range of 1–9, dropping slightly to 3 with a range of 1–6 at 5 h (Fig. 2B). Thus the percentage of infected target cells and the number of nuclear vDNA spots reached a maximum at 3 h, presumably representing a plateau in the nuclear import of proviral DNA. These data are consistent with those of Del Portillo et al. (2011) who observed an average of 3.82 proviral copies 30 h after co-culture, with the added advantage that our system excludes cell-free vDNA signal as none is detectable within 6 h (Fig. 5 and Martin et al. (2010).

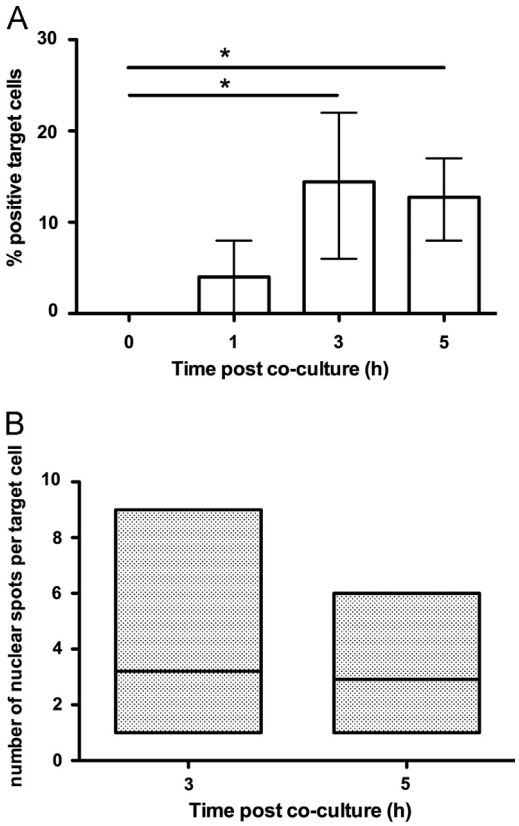

Fig. 2. Quantification of vDNA in target cell nuclei. Random fields from cocultures of Jkt_{IIIB} and A301.R5 cells were evaluated for the presence of vDNA in target cell nuclei revealed by FISH at the times shown. (A) The bars represent the percentage of all target cells containing one or more vDNA spots. Error bars represent 1 SD. Statistical significance was calculated using ANOVA with Bonferroni multiple comparison post-test comparing each to time point 0 h, $^{*}p = < 0.05$. (B) The number of vDNA spots was counted in each positive target cell nucleus, and the results presented as range and mean value.

HIV-1 cell-to-cell transfer results in vDNA integration

Although the FISH results revealed proviral nuclear import, nuclear localization of vDNA does not demonstrate integration. We therefore adopted a semi-quantitative (q)PCR method that specifically amplifies integrated vDNA, and applied this to conjugates of Jkt_{IIIB} or $Jkt.R5_{Ba\text{-}L}$ and A301.R5 target or A201 control cells. The method was based on the linker-primer method of Vandegraaff et al. (2001) that relies upon restriction digestion of cellular DNA with *Nla*III for which a conserved restriction site also contained within the HIV-1 LTR exists. The advantage of this approach over the Alu PCR method is that the *Nla*III restriction site occurs more frequently (< 1 kb) in the genome than *Alu* sites which occur once every 2.5 kb (Grover et al., 2004), therefore the distance between an HIV-1 integrant and a *Nla*III site will be less allowing detection of more integration events (Mantovani et al., 2006). Enzymatic digestion with *Nla*III results in a 5′ overhang that can be ligated with a linker that contains a primer for the LTR, allowing amplification of integrated HIV-1 sequences. The original method was modified to allow qPCR amplification of integrated LTR subsequent to the nested PCR reaction, allowing semi-quantification of the final product. All signals were normalized to the baseline level of signal produced in the HIV-1-infected T cells-A201 control target cell conjugates at equivalent time points. At 0 h a very low level of integrated vDNA was detected in the Jkt_{IIIB}-A301.R5 conjugates. However, over time the value increased (Fig. 3), reflecting newly integrated vDNA in the A301.R5 target cells. If a maximum of 15% of target cells are infected (Fig. 2A), this suggests that at 6 h each infected target cell may contain an average of 1 integrated provirus. However this is likely to be an underestimate since the qPCR method we have used will lose efficiency relative to amplicon length, which will vary depending upon the site of integration. When the infected and target cells were separated by a transwell the level of integration remained significantly lower ($p < 0.001$ at 24 h) than the cell-to-cell co-culture throughout the time course, further confirming that cell-to-cell contact increases proviral DNA transfer (Chen et al., 2007; Del Portillo et al., 2011; Martin et al., 2010; Sourisseau et al., 2007). When the co-culture was performed in the presence of the integrase inhibitor Raltegravir the level of integrated vDNA remained low throughout the time course confirming the specificity of the integration PCR assay. Although the signal in the presence of Raltegravir increased modestly over time, this was not significant. We conclude that this is probably detection of 2LTR circles, which increase in the presence of Raltegravir (Buzon et al., 2010). Although these 2LTR circles cannot be amplified by the first round linker PCR reaction of the integration assay (Vandegraaff et al., 2001) they are still amplifiable by the second round nested reaction.

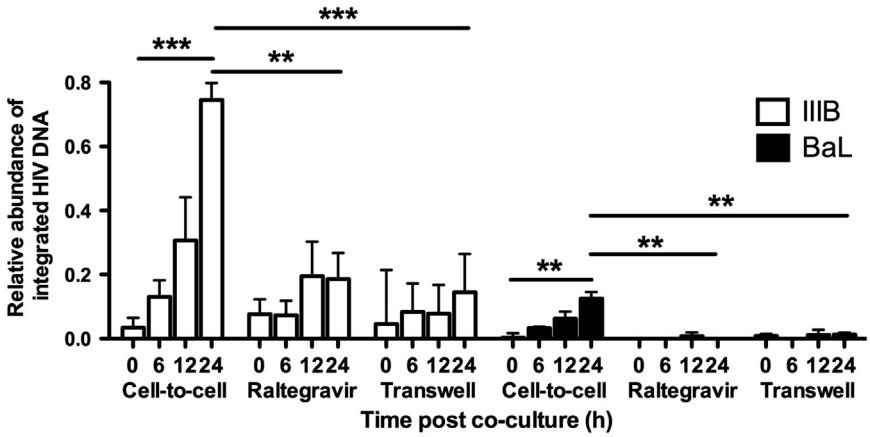

Fig. 3. qPCR for integrated proviral DNA. (A) Jurkat cells infected with HIV-$1_{Ba\text{-}L}$ or HIV-1_{IIIB} were mixed with target A201 or A301.R5 cells for the times indicated in the presence or absence of Raltegravir and with and without transwell separation, followed by lysis and extraction of DNA, then digestion to create fragments. Semi-quantitative PCR was carried out using primers designed to selectively amplify integrated forms of HIV-1 DNA, and *β-globin*, as detailed in the methods. Values were normalised to *β-globin* copy number and at each time point the control result using non-susceptible A201 was subtracted from the A301.R5 test result to remove any signal present in donor cells. Results are expressed as abundance of HIV-1 copies per cell. Bars represent mean values from up to four independent experiments, and error bars represent SEM. Statistical significance was calculated using ANOVA with Bonferroni multiple comparison post-test comparing time points within the cell-to-cell samples and the 24 h time point between with cell-to-cell, Raltegravir treated and the cell-free transwell samples. $^{*}p = < 0.05$, $^{**}p = < 0.01$, $^{***}p = < 0.001$.

A similar pattern of integration was obtained for the Jkt.$R5_{Ba\text{-}L}$-A301.R5 conjugates (Fig. 3), which showed increased numbers of copies of integrated DNA over time in the cell-to-cell conjugates, which were completely abolished if the cells were separated by a transwell or the cell-to-cell conjugates were co-cultured in the presence of Raltegravir. We saw a much more modest signal in the Jkt.$R5_{Ba\text{-}L}$-A301.R5 conjugates than the Jkt_{IIIB}-A301.R5 conjugates which cannot be explained by differences in target cell co-receptor expression or donor cell infection level, which were comparable (Fig. 4). These observations support our previous results showing that R5 HIV-1 infection kinetics via VS are slower than those of X4 HIV-1 (Martin et al., 2010).

HIV-1 cell-to-cell transfer results in synthesis of vRNA

Although proviral integration indicates that a cell is stably infected by HIV-1, this may not necessarily lead to a productive infection. To investigate productivity of target cell infection, we measured de-novo synthesis of total vDNA and vRNA using qPCR with primers against HIV-1 *pol* as previously described (Jolly et al., 2007a, 2007b; Martin et al., 2010). All signals were normalized to the baseline level of signal produced in HIV-1-infected Jurkats-A301.R5 conjugates in the presence of the blocking antibody 13B8.2 at equivalent time points. Fig. 5A shows increasing HIV-1_{IIIB} *pol* vDNA signal in target A301.R5 cells relative to β-globin that became detectable at 6 h and was significantly greater than starting levels by 24 h post-cell mixing. We hypothesize that this increase is due to vRNA transfer across the synapse, which then undergoes reverse transcription and integration (Fig. 3). HIV-1_{IIIB} RNA levels increased over time similarly to those of vDNA but with a delay, since there was no detectable increase over starting values at 12 h, but a clear increase was observed at 24 h. Most likely the increase in vRNA results from transcription of integrated provirus. The delay in vRNA production compared to vDNA production is in line with viral replication kinetics whereby vRNA is amplified from integrated vDNA. HIV-$1_{Ba\text{-}L}$ showed a similar pattern (Fig. 5B), with vDNA detectable at 12 h post-cell mixing which reached significance at 24 h and vRNA detectable at 24 h. At these early time points we consider that we are not detecting a spreading infection with a significant cell-free infectious contribution, as no integration signal above background was detected in the presence of a transwell at 24 h (Fig. 3), and we have previously shown a lack of vDNA signal above background in similar cell-free infection systems at 24 h (Martin et al., 2010).

Discussion

Here we show that cell-to-cell infection of $CD4^+$ T cells across VS results in de-novo production of vDNA reverse transcripts, a proportion of which integrates into the target cell chromatin with greater efficiency than that seen following cell-free infection. The kinetics and levels of vDNA detection we find are consistent with previous studies that quantified the appearance of de-novo vDNA following both cell-free and cell-to-cell infection. Vandegraaff et al. (2001) showed detection of proviral integrants at 4 h post high-multiplicity infection of a $CD4^+$ T cell line, similar to our first significant detection at 6 h and Del Portillo et al. (2011) showed an average of 3.82 proviral copies per cell in line with our estimated 3.4 proviral copies. Analysis of vRNA revealed a time-dependent increase consistent with a productive infection of the target cells.

These results add weight to the concept that HIV-1 spread across T cell VS results in productive infection of $CD4^+$ T cells, and provide direct evidence to support the idea that VS-mediated spread of HIV-1 is likely to result in super-infection of individual $CD4^+$ T cells leading to multiple integration events. Multiple HIV-1 proviruses per cell have been observed ex-vivo by FISH analysis in $CD4^+$ splenocytes in situ (Jung et al., 2002), and inferred by sequence analysis of viral quasispecies within individual $CD4^+$ T cells (Jung et al., 2002) and in sections of spleens (Gratton et al., 2000) from HIV-1-infected individuals. A high proportion of HIV-1-infected T cells containing multiple proviral genomes is consistent with the high multiplicity of infection imparted to a permissive target cell by directed cell-to-cell spread (Dimitrov et al., 1993; Dixit and Perelson, 2004; Martin et al., 2010), as opposed to the predicted low multiplicity imparted by cell-free infection that is limited by fluid-phase diffusion and a high rate of viral dissociation from the target cell (Platt et al., 2010). Our data are therefore in line with models implying that cell-to-cell spread of HIV-1 in man and SIV in non-human primates is a dominant mode of viral dissemination within secondary lymphoid tissue (Grossman et al., 1998; Haase, 1999; Reilly et al., 2002). In this context it has recently been shown in a bone marrow/liver/thymus (BLT) humanized mouse model that HIV-1 induces a partial reduction in the motility of infected T cells allowing more time for VS to form while not significantly

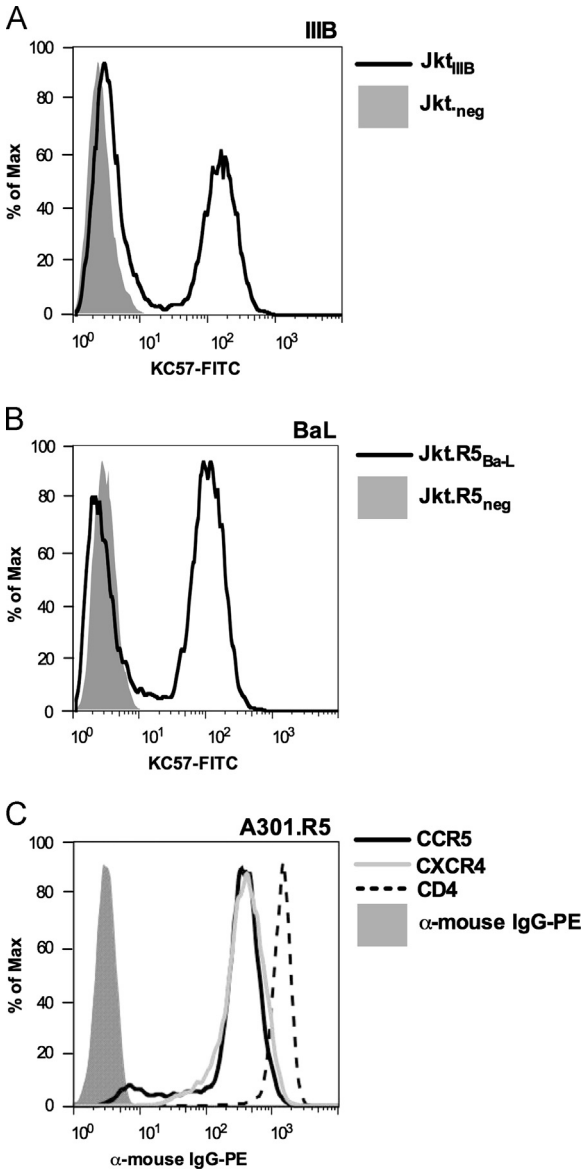

Fig. 4. Cell surface expression level or HIV-1 receptor and co-receptors and infection level of donor cells. (A) Infected Jkt_{IIIB} and uninfected control Jurkat cells were stained with KC57-FITC for HIV-1 Gag detection. (B) Infected $Jkt.R5_{Ba-L}$ and uninfected control Jurkat cells were stained with KC57-FITC for HIV-1 Gag detection. (C) Target A301.R5 cells were stained for CD4, CXCR4 and CCR5. As a control A301.R5 cells were stained with secondary antibody only.

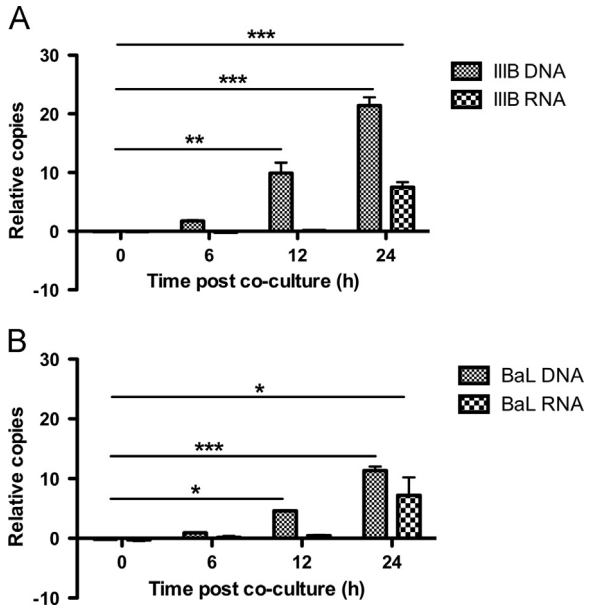

Fig. 5. qPCR for vDNA and vRNA. (A) Jkt_{IIIB} were mixed with target A301.R5 cells for the times indicated, followed by lysis and extraction of total DNA and RNA. Quantitative PCR was carried out on DNA using *pol*-specific primers and normalized to the signal obtained with *β-globin* primers. The amount of HIV-1_{IIIB} RNA was assayed by qRT-PCR using *pol* specific primers normalized against cellular β-actin. The means of 3 independent experiments normalised to the 0 h time point in the presence of 13B8.2 are shown, error bars represent SEM. Statistical significance was calculated using ANOVA with Bonferroni multiple comparison post-test comparing each to 0 h. $^{**}p = < 0.01$, $^{***}p = < 0.001$. (B) As in (A) except that $Jkt.R5_{BaL}$ were mixed with A301.R5 cells for the times indicated. The means of 3 independent experiments normalized to the 0 h time point in the presence of 13B8.2 are shown. Statistical significance was calculated using ANOVA with Bonferroni multiple comparison post-test comparing each to 0 h. $^{*}p = < 0.05$, $^{***}p = < 0.001$.

reducing the dissemination of these T cells throughout the body (Murooka et al., 2012). This observation suggests that the formation of VS and the subsequent viral transfer is a characteristic of optimal in vivo HIV-1 infection. These findings not only have implications for potential multiple integration events leading to recombination amongst distinct viral genomes, but also for reduced sensitivity of HIV-1 to antiretroviral therapy, which decreases as a function of increasing multiplicity (Sigal et al., 2011).

A caveat of the current analysis is that we have used transformed $CD4^+$ T cell lines as donor and target cells. Although cell lines are generally accepted as appropriate model systems for analysis of HIV-1 cell-to-cell transfer (Blanco et al., 2004; Chen et al., 2007; Hubner et al., 2009; Martin et al., 2010; Mazurov et al., 2010; Puigdomenech et al., 2009; Sato et al., 1992), their constitutively activated status means that they are poorly representative of naïve and quiescent memory $CD4^+$ T cell populations. In this case the particular cell lines used have previously been shown to form VS with the same gp120-receptor and adhesion molecule interactions as those seen in primary cell VS (Jolly et al., 2007a; Rudnicka et al., 2009), giving confidence that our data are generally representative of a T cell VS. Since HIV-1 reverse transcription, vDNA stability, proviral integration and subsequent viral replication steps are dependent upon T cell activation state (Arfi et al., 2009; Manganaro et al., 2010; Vatakis et al., 2009; Zhou et al., 2005), however, future studies should consider the role of cell-to-cell spread in the infection of primary $CD4^+$ T cells in various states of activation. Moreover, since VS can form between cells other than T cells, and have been described for HIV-1 spread between DCs and T cells (Larsson, 2005) and macrophages and T cells (Groot et al., 2008) analysis of integration dynamics in these systems will be revealing.

Conclusions

The results presented here reveal that viral spread across a T cell to T cell VS leads to the transfer of multiple copies of HIV-1 vRNA into the target cell, followed by reverse transcription, integration and establishment of a productive infection. This not only confirms that HIV-1 cell-to-cell spread is highly efficient and productive, but also provides a mechanism for recombination between distinct HIV-1 genomes within multiply infected cells.

Materials and methods

Cells and viruses

Jurkat E6.1 and Jurkat.Tat.R5 cells (Morcock et al., 2005) were from the NIBSC Centre for AIDS Reagents (CFAR) and were maintained in

growth medium (GM): RPMI+10% foetal calf serum and 100 U/mL penicillin and 100 μg/mL streptomycin. Jurkat.Tat.R5 cells were maintained in 1 mg/mL G418 prior to infection. Virus isolates HIV-1_{IIIB} and HIV-$1_{Ba\text{-}L}$ were obtained from the CFAR, (NIBSC) UK. Jurkat E6.1 cells were infected with HIV-1_{IIIB} (Jkt_{IIIB}), and Jurkat.Tat.R5 cells were infected with HIV-$1_{Ba\text{-}L}$ (Jkt.$R5_{Ba\text{-}L}$) for 7–10 days at which time Env and Gag expression were highest as measured by flow cytometry as previously described (Martin et al., 2010) (Fig. 4A and B shows Gag expression at day 7). Target cells were A301.R5, which express CD4, CXCR4 and CCR5 (Fig. 4C) and are therefore permissive to both X4 and R5 HIV-1 infection, and control A201 cells which lack CD4 and CCR5 (Jolly et al., 2007a, 2007b; Martin et al., 2010). Both were maintained in GM; A301.R5 cells were also maintained in 1 mg/mL G418 prior to infection.

Immunofluorescent labelling and laser scanning confocal microscopy (LSCM)

Jkt.$R5_{Ba\text{-}L}$ cells were mixed with target A301.R5 cells pre-labelled with the non-blocking CD4 mAb L120 (CFAR) and co-cultured for the times shown prior to fixation in 1% formaldehyde as described previously (Martin et al., 2010). Cells were labelled with mAb to Env (2G12, CFAR) and rabbit anti-Gag p24/p17 (CFAR), counterstained with anti-mouse Alexa 488 (Invitrogen, UK), anti-human-TRITC and anti-rabbit Cy5 (Jackson-Immunotech, UK) and mounted on glass slides using Pro-Long Gold (Invitrogen, UK). Images were acquired using a Zeiss Pascal Axiovert 200M using sequential capture to avoid channel cross-talk, and processed using Adobe Photoshop CS2.

Fluorescence in-situ hybridization (FISH)

The DIG-Nick Translation mix (Roche) was used to generate digoxigenin-11-dUTP-labelled probes from the NL4.3 HIV-1 plasmid. DIG-Nick translation mix (4 μL) was added to 1 μg of pNL4.3 in 16 μL distilled (d)H_2O. The sample was incubated for 90 min at 15 °C then placed on ice. At various times 3 μL aliquots of the sample were mixed with loading buffer, denatured at 95 °C for 3 min, cooled for 3 min and run on a 1% agarose gel to determine fragment lengths of the labelled probe. Probe lengths between 200 and 500 nucleotides were diluted in 1 μL 0.5 M EDTA (pH 8.0) and the sample heated to 65 °C for 10 min. Unincorporated free fluorophore-dNTPs were removed with the Qiagen PCR purification kit. Gene frames (1 × 1 cm^2, AbGene) on poly-L-Lysine-coated glass slides were washed with distilled (d)H_2O and air-dried. Target A301.R5 cells were labelled with cell tracker orange (Invitrogen), washed and resuspended in RPMI-1640 with 1% FCS. Infected cells (2×10^5 Jkt_{IIIB} or Jkt.$R5_{Ba\text{-}L}$) were washed in PBS and mixed with an equal number of labelled A301.R5 cells. and 100 μL of the cell mixture was applied to the poly-L-lysine treated slides. Slides were incubated at 37 °C in high humidity for 1, 3, and 6 h, fixed with 4% paraformaldehyde in PBS for 15 min at 4 °C and cells permeabilized with 0.2% Triton-X100 in PBS for 10 min at RT. For detection of DNA only cells were treated with 100 μg/mL RNAase for 30 min at 37 °C before adding 2 × SSC for 5 min at RT. Slides were dehydrated at −20 °C through an ethanol series and air dried. Probe mix was 10 ng digoxigenin-labelled probe in 50% formamide, 2 × SSC, 10% dextran sulphate, 1 μg salmon sperm DNA, 10 μg yeast tRNA and 5 μg Cot1 DNA made up to a total of 15 μL per slide in dH_2O. Probe mix was added to the slides and sealed before denaturation at 94 °C for 4 min. Slides were placed at 37 °C for 3 h, unsealed and washed at 37 °C: 2 × 15 min in 55% formamide, 2 × SSC buffer, 10 min in 2 × SSC buffer 2 × 5 min 0.25 × SSC buffer. Slides were blocked in 1% BSA, 4 × SSC buffer with 0.1% Tween-20. The probe was detected with 1:25,000 sheep anti-digoxigenin antibody (Thermo Scientific) and 1:500 anti-sheep Alexa 488. Slides were washed 3 × in 0.1% tween, 2 × SSC buffer containing 1:5000 TOTO-1 (Invitrogen) and mounted in Vectashield (Vectorlabs). For quantification of HIV-1 proviral copies by FISH, random fields were scored for number of target cells, number of target cells with spots, and number of spots per positive cell. Results were expressed as percentage of target cells with spots and number of spots per positive target cell.

qPCR for integrated proviral DNA

The method is based on (Vandegraaff et al., 2001). Primers were designed to detect both HIV-1_{IIIB} and HIV-$1_{Ba\text{-}L}$ sequences from the LANL database (www.hiv.lanl.web). Primer sequences were as follows: LPNV–TCATGATCAATGGGACGATCACATG, U3NV–GTGTAACAAG-CAGTTGTTCTCTCC, HIVuniversalF–GGAAGGGCTAATTCACTC, HIVuniversalR–CACCATCCAAAGGTCAGTGG, β-globin-S–AACTGGGCATGTGGA GACAGA, β-globin AS–CTAAGGGTGGGAAAATAGACCAATAG. For each sample, 5×10^5 infected cells were mixed with 5×10^5 target A301.R5 cells in 300 μL GM per well of 96-well plates. Plates were incubated at 37 °C in 5% CO_2. At appropriate time points cells were pelleted, supernatant aspirated, and pellets frozen at −80 °C for DNA extraction using DNeasy Blood and Tissue Kit (Qiagen). For the first restriction digest, 10 × OPA+ buffer was prepared: 1 M potassium acetate, 250 mM tris-acetate, 100 mM magnesium acetate, 5 mM β-mercaptoethanol, 100 μg/mL BSA in dH_2O. Isolated chromosomal DNA (2.5 μL) was digested to completion for 3 h at 37 °C with 20 U of *Bgl*II (New England Biolabs) in 2 × OPA+ buffer in 20 μL. The second digest was performed in a volume of 40 μL for 3 h at 37 °C in a final buffer of 1 × OPA+, 100 μg/mL BSA, 1 mM dithiothreitol and 10 U of *Nla*III (New England Biolabs). Two nucleotides (G and A) of the *Bgl*II overhang generated by digestion were filled in by adjusting the sample to final concentrations of 7.5 mM dithiothreitol, 0.25 mM dGTP (Promega), 0.25 mM dATP (Promega) and 5 U of Klenow (New England Biolabs) in 50 μL for 30 min at 37 °C, and excess dNTPs were removed with a QiaQuick PCR Clean-up kit (Qiagen). Linker ligation was carried out by resuspending DNA in 10 μL ligation buffer (1 × in final volume, New England Biolabs) and 50 pmol of LPNV made up to 100 μL in dH_2O. Samples were heated to 60 °C for 10 min to anneal the primer, then snap-cooled on ice to minimize inter- and intramolecular ligation of *Nla*III fragments. T4 DNA ligase (400 U, New England Biolabs) was added and samples incubated overnight at 16 °C. For the first round PCR, 1 × PCR Buffer II (Applied Biosystems) was mixed with 2 mM $MgCl_2$ and 0.2 mM deoxynucleoside triphosphates (dNTPs) (Promega). 50 pmol of LPNV and 100 pmol of U3NV were added along with 5 U of AmpliTaq Gold DNA Polymerase (Applied Biosystems) and the final volume was adjusted to 100 μL. The PCR was cycled as follows: denaturation at 95 °C, 12 min; 22 cycles, 94 °C; denaturation 30 s, primer annealing at 58 °C, 30 s, extension 72 °C, 1 min; final extension 72 °C, 10 min. Nested qPCR was as follows. 6 μM each forward and reverse primers were mixed with 1 × MESA Green qPCR mastermix (Eurogentec) and a standard curve constructed using ABI7500 software. All qPCRs were cycled on the Applied Biosystems 7500 as follows: 50 °C, 2 min; 95 °C, 10 min; 40 cycles, 95 °C, 15 s followed by 60 °C, 1 min. Values were normalized to *hbb* copy number in the starting sample, determined using SYBR green detection with β-globin-S and β-globin-AS primers in place of HIV primers.

qPCR for viral (v)RNA and vDNA

Jkt.$R5_{Ba\text{-}L}$ and Jkt_{IIIB} cells were co-cultured with A301.R5 cells for the times shown ± 10 μg/mL blocking CD4 antibody 13B8.2 (Beckman Coulter). At each time point cells were pelleted, supernatant discarded and DNA and RNA extracted using the Illustra TriplePrep Kit (GE Healthcare). HIV-1 DNA was quantified using the HIV-$1_{Ba\text{-}L}$ *pol* primer/probe set (Martin et al., 2010) and the *β*-globin internal control primer/probe set. HIV-1 RNA was quantified using Superscript III First Strand Synthesis SuperMix

(Invitrogen) for cDNA production followed by the HIV-1 *pol* primer probe set and the β-*actin* internal control primer set (Eurogentec) with SybrGreen detection. As a control for DNA contamination, cDNA production was carried out in the absence of reverse transcriptase and the resulting mix was used in the qPCR reaction: no signal was detected confirming the absence of any DNA contamination (data not shown).

Statistical analysis

FISH results were analysed using ANOVA with Bonferroni multiple comparison post-test comparing all samples to the 0 h time point and an unpaired two-tailed *t*-test comparing the 3 and 5 h time points. Results of the integration PCR, the qPCR and the qRT-PCR on the integrated DNA, the total vDNA and the vRNA, respectively, were analysed using ANOVA with Bonferroni multiple comparison post-test to compare all samples to the 0 h time point unless otherwise stated in the figure legends.

Authors' contributions

NM, RR, IM and EJ devised experimental methods, developed techniques and carried out the experimental work. QJS and NM conceived of the project, and QJS, RR and NM wrote the manuscript.

Acknowledgments

This study was supported by Medical Research Council award G0901732 and Dormeur Investment Service Ltd. QS is a Jenner Institute Investigator and a James Martin Senior Fellow.

References

Arfi, V., Lienard, J., Nguyen, X.N., Berger, G., Rigal, D., Darlix, J.L., Cimarelli, A., 2009. Characterization of the behavior of functional viral genomes during the early steps of human immunodeficiency virus type 1 infection. J. Virol. 83, 7524–7535.

Blanco, J., Bosch, B., Fernandez-Figueras, M.T., Barretina, J., Clotet, B., Este, J.A., 2004. High level of coreceptor-independent HIV transfer induced by contacts between primary CD4 T cells. J. Biol. Chem. 279, 51305–51314.

Buzon, M.J., Massanella, M., Llibre, J.M., Esteve, A., Dahl, V., Puertas, M.C., Gatell, J.M., Domingo, P., Paredes, R., Sharkey, M., Palmer, S., Stevenson, M., Clotet, B., Blanco, J., Martinez-Picado, J., 2010. HIV-1 replication and immune dynamics are affected by raltegravir intensification of HAART-suppressed subjects. Nat. Med. 16, 460–465.

Chen, P., Hubner, W., Spinelli, M.A., Chen, B.K., 2007. Predominant mode of human immunodeficiency virus transfer between T cells is mediated by sustained Env-dependent neutralization-resistant virological synapses. J. Virol. 81, 12582–12595.

Clouse, K.A., Powell, D., Washington, I., Poli, G., Strebel, K., Farrar, W., Barstad, P., Kovacs, J., Fauci, A.S., Folks, T.M., 1989. Monokine regulation of human immunodeficiency virus-1 expression in a chronically infected human T cell clone. J. Immunol. 142, 431–438.

Del Portillo, A., Tripodi, J., Najfeld, V., Wodarz, D., Levy, D.N., Chen, B.K., 2011. Multiploid inheritance of HIV-1 during cell-to-cell infection. J. Virol. 85, 7169–7176.

Dimitrov, D.S., Willey, R.L., Sato, H., Chang, L.J., Blumenthal, R., Martin, M.A., 1993. Quantitation of human immunodeficiency virus type 1 infection kinetics. J. Virol. 67, 2182–2190.

Dixit, N.M., Perelson, A.S., 2004. Multiplicity of human immunodeficiency virus infections in lymphoid tissue. J. Virol. 78, 8942–8945.

Gratton, S., Cheynier, R., Dumaurier, M.J., Oksenhendler, E., Wain-Hobson, S., 2000. Highly restricted spread of HIV-1 and multiply infected cells within splenic germinal centers. Proc. Natl. Acad. Sci. USA 97, 14566–14571.

Groot, F., Welsch, S., Sattentau, Q.J., 2008. Efficient HIV-1 transmission from macrophages to T cells across transient virological synapses. Blood 111, 4660–4663.

Grossman, Z., Feinberg, M.B., Paul, W.E., 1998. Multiple modes of cellular activation and virus transmission in HIV infection: a role for chronically and latently infected cells in sustaining viral replication. Proc. Natl. Acad. Sci. USA 95, 6314–6319.

Grover, D., Mukerji, M., Bhatnagar, P., Kannan, K., Brahmachari, S.K., 2004. Alu repeat analysis in the complete human genome: trends and variations with respect to genomic composition. Bioinformatics 20, 813–817.

Haase, A.T., 1999. Population biology of HIV-1 infection: viral and CD4+ T cell demographics and dynamics in lymphatic tissues. Annu. Rev. Immunol. 17, 625–656.

Hubner, W., McNerney, G.P., Chen, P., Dale, B.M., Gordon, R.E., Chuang, F.Y., Li, X.D., Asmuth, D.M., Huser, T., Chen, B.K., 2009. Quantitative 3D video microscopy of HIV transfer across T cell virological synapses. Science 323, 1743–1747.

Jolly, C., Kashefi, K., Hollinshead, M., Sattentau, Q.J., 2004. HIV-1 cell to cell transfer across an Env-induced, actin-dependent synapse. J. Exp. Med. 199, 283–293.

Jolly, C., Mitar, I., Sattentau, Q.J., 2007a. Adhesion molecule interactions facilitate human immunodeficiency virus type 1-induced virological synapse formation between T cells. J. Virol. 81, 13916–13921.

Jolly, C., Mitar, I., Sattentau, Q.J., 2007b. Requirement for an intact T-cell actin and tubulin cytoskeleton for efficient assembly and spread of human immunodeficiency virus type 1. J. Virol. 81, 5547–5560.

Jung, A., Maier, R., Vartanian, J.P., Bocharov, G., Jung, V., Fischer, U., Meese, E., Wain-Hobson, S., Meyerhans, A., 2002. Recombination: multiply infected spleen cells in HIV patients. Nature 418, 144.

Larsson, M., 2005. HIV-1 and the hijacking of dendritic cells: a tug of war. Springer Seminars in Immunopathology 26, 309–328.

Manganaro, L., Lusic, M., Gutierrez, M.I., Cereseto, A., Del Sal, G., Giacca, M., 2010. Concerted action of cellular JNK and Pin1 restricts HIV-1 genome integration to activated CD4+ T lymphocytes. Nat. Med. 16, 329–333.

Mantovani, J., Holic, N., Martinez, K., Danos, O., Perea, J., 2006. A high throughput method for genome-wide analysis of retroviral integration. Nucl. Acids Res. 34, e134.

Martin, N., Welsch, S., Jolly, C., Briggs, J.A., Vaux, D., Sattentau, Q.J., 2010. Virological synapse-mediated spread of human immunodeficiency virus type-1 between T cells is sensitive to entry inhibition. J. Virol..

Mazurov, D., Ilinskaya, A., Heidecker, G., Lloyd, P., Derse, D., 2010. Quantitative comparison of HTLV-1 and HIV-1 cell-to-cell infection with new replication dependent vectors. PLoS Pathog. 6, e1000788.

Morcock, D.R., Thomas, J.A., Gagliardi, T.D., Gorelick, R.J., Roser, J.D., Chertova, E.N., Bess Jr., J.W., Ott, D.E., Sattentau, Q.J., Frank, I., Pope, M., Lifson, J.D., Henderson, L.E., Crise, B.J., 2005. Elimination of retroviral infectivity by N-ethylmaleimide with preservation of functional envelope glycoproteins. J. Virol. 79, 1533–1542.

Murooka, T.T., Deruaz, M., Marangoni, F., Vrbanac, V.D., Seung, E., von Andrian, U.H., Tager, A.M., Luster, A.D., Mempel, T.R., 2012. HIV-infected T cells are migratory vehicles for viral dissemination. Nature 490, 283–287.

Piguet, V., Sattentau, Q., 2004. Dangerous liaisons at the virological synapse. J. Clin. Invest. 114, 605–610.

Platt, E.J., Kozak, S.L., Durnin, J.P., Hope, T.J., Kabat, D., 2010. Rapid dissociation of HIV-1 from cultured cells severely limits infectivity assays, causes the inactivation ascribed to entry inhibitors, and masks the inherently high level of infectivity of virions. J. Virol. 84, 3106–3110.

Puigdomenech, I., Massanella, M., Cabrera, C., Clotet, B., Blanco, J., 2009. On the steps of cell-to-cell HIV transmission between CD4 T cells. Retrovirology 6, 89.

Reilly, C., Schackler, T., Haase, A.T., Wietgrefe, S., Krason, D., 2002. The clustering of infected SIV cells in lymphatic tissue. J. Amer. Statist. Assoc. 97, 943–954.

Rudnicka, D., Feldmann, J., Porrot, F., Wietgrefe, S., Guadagnini, S., Prevost, M.C., Estaquier, J., Haase, A.T., Sol-Foulon, N., Schwartz, O., 2009. Simultaneous cell-to-cell transmission of human immunodeficiency virus to multiple targets through polysynapses. J. Virol. 83, 6234–6246.

Ruggiero, E., Bona, R., Muratori, C., Federico, M., 2008. Virological consequences of early events following cell–cell contact between human immunodeficiency virus type 1-infected and uninfected CD4+ cells. J. Virol. 82, 7773–7789.

Sato, H., Orenstein, J., Dimitrov, D., Martin, M., 1992. Cell-to-cell spread of HIV-1 occurs within minutes and may not involve the participation of virus particles. Virology 186, 712–724.

Sattentau, Q., 2008. Avoiding the void: cell-to-cell spread of human viruses. Nat. Rev. Microbiol. 6, 815–826.

Sigal, A., Kim, J.T., Balazs, A.B., Dekel, E., Mayo, A., Milo, R., Baltimore, D., 2011. Cell-to-cell spread of HIV permits ongoing replication despite antiretroviral therapy. Nature 477, 95–98.

Sourisseau, M., Sol-Foulon, N., Porrot, F., Blanchet, F., Schwartz, O., 2007. Inefficient human immunodeficiency virus replication in mobile lymphocytes. J. Virol. 81, 1000–1012.

Vandegraaff, N., Kumar, R., Burrell, C.J., Li, P., 2001. Kinetics of human immunodeficiency virus type 1 (HIV) DNA integration in acutely infected cells as determined using a novel assay for detection of integrated HIV DNA. J. Virol. 75, 11253–11260.

Vasiliver-Shamis, G., Tuen, M., Wu, T.W., Starr, T., Cameron, T.O., Thomson, R., Kaur, G., Liu, J., Visciano, M.L., Li, H., Kumar, R., Ansari, R., Han, D.P., Cho, M.W., Dustin, M.L., Hioe, C.E., 2008. Human immunodeficiency virus type 1 envelope gp120 induces a stop signal and virological synapse formation in noninfected CD4+ T cells. J. Virol. 82, 9445–9457.

Vasiliver-Shamis, G., Cho, M.W., Hioe, C.E., Dustin, M.L., 2009. Human immunodeficiency virus type 1 envelope gp120-induced partial T-cell receptor signaling creates an F-actin-depleted zone in the virological synapse. J. Virol. 83, 11341–11355.

Vasiliver-Shamis, G., Dustin, M.L., Hioe, C.E., 2010. HIV-1 virological synapse is not simply a copycat of the immunological synapse. Viruses 2, 1239–1260.

Vatakis, D.N., Nixon, C.C., Bristol, G., Zack, J.A., 2009. Differentially stimulated CD4+ T cells display altered human immunodeficiency virus infection kinetics: implications for the efficacy of antiviral agents. J. Virol. 83, 3374–3378.

Wu, Y., 2008. The second chance story of HIV-1 DNA: unintegrated? Not a problem!. Retrovirology 5, 61.

Zhou, Y., Zhang, H., Siliciano, J.D., Siliciano, R.F., 2005. Kinetics of human immunodeficiency virus type 1 decay following entry into resting CD4+ T cells. J. Virol. 79, 2199–2210.